Protein Cell 2012, 3(2): 123–131
DOI 10.1007/s13238-012-2026-5

Protein & Cell

RESEARCH ARTICLE

Crystal structures of D-psicose 3-epimerase from *Clostridium cellulolyticum* H10 and its complex with ketohexose sugars

Hsiu-Chien Chan[1*], Yueming Zhu[1*], Yumei Hu[1], Tzu-Ping Ko[2], Chun-Hsiang Huang[1], Feifei Ren[1], Chun-Chi Chen[3], Yanhe Ma[1], Rey-Ting Guo[1] ✉, Yuanxia Sun[1] ✉

[1] Industrial Enzymes National Engineering Laboratory, Institute of Industrial Biotechnology, Chinese Academy of Sciences, Tianjin 300308, China
[2] Institute of Biological Chemistry, Academia Sinica, Taipei 115, Taiwan, China
[3] CAS Key Laboratory of Pathogenic Microbiology and Immunology, Institute of Microbiology, Chinese Academy of Sciences, Beijing 100101, China
✉ Correspondence: guo_rt@tib.cas.cn (R.-T. Guo), sun_yx@tib.cas.cn (Y. Sun)
Received January 22, 2012 Accepted February 5, 2012

ABSTRACT

D-Psicose 3-epimerase (DPEase) is demonstrated to be useful in the bioproduction of D-psicose, a rare hexose sugar, from D-fructose, found plenty in nature. *Clostridium cellulolyticum* H10 has recently been identified as a DPEase that can epimerize D-fructose to yield D-psicose with a much higher conversion rate when compared with the conventionally used DTEase. In this study, the crystal structure of the *C. cellulolyticum* DPEase was determined. The enzyme assembles into a tetramer and each subunit shows a $(\beta/\alpha)_8$ TIM barrel fold with a Mn^{2+} metal ion in the active site. Additional crystal structures of the enzyme in complex with substrates/products (D-psicose, D-fructose, D-tagatose and D-sorbose) were also determined. From the complex structures of *C. cellulolyticum* DPEase with D-psicose and D-fructose, the enzyme has much more interactions with D-psicose than D-fructose by forming more hydrogen bonds between the substrate and the active site residues. Accordingly, based on these ketohexose-bound complex structures, a C3-O3 proton-exchange mechanism for the conversion between D-psicose and D-fructose is proposed here. These results provide a clear idea for the deprotonation/protonation roles of E150 and E244 in catalysis.

KEYWORDS D-psicose 3-epimerase, ketohexose, complex structure

INTRODUCTION

D-Psicose is poorly absorbed in digestive tract and produces almost no energy, and thus is a valuable source for preparing low-calorie sweetener as food additive (Matsuo et al., 2002). In diabetic patients, the supplemental D-psicose might be helpful in preventing post prandial hyperglycemia (Matsuo et al., 2001; Matsuo and Izumori, 2006). D-Psicose is a rare sugar that exists in small quantities in nature and is difficult to synthesize chemically. Therefore the most promising approach to produce D-psicose is to use enzymatic reaction (Granström et al., 2004). The *Pseudomonoas cichorii* D-tagatose 3-epimerase (DTEase), which belongs to the DTEase family, can convert D-tagatose and D-fructose to D-sorbose and D-psicose, respectively, by catalyzing the epimerization at carbon-3 (C3) position (Izumori, 1995, 2002; Kim et al., 2008; Samuel and Tanner, 2002) (Fig. 1). More recently, a putative *Agrobacterium tumefaciens* DTEase has been renamed as DPEase because it converts D-psicose more efficiently (Kim et al., 2006a). The bioconversion rate of D-psicose for the enzyme is 32.9%, higher than the 20% for that of *P. cichorii* DTEase (Itoh et al., 1994). The newly identified DPEase attracts enormous commercial interest and would be widely used for rare sugar production in the future.

The epimerization activity of DTEase from *P. cichorii* was the highest for D-tagatose, and it decreased with the order of

*These authors contributed equally to the work.

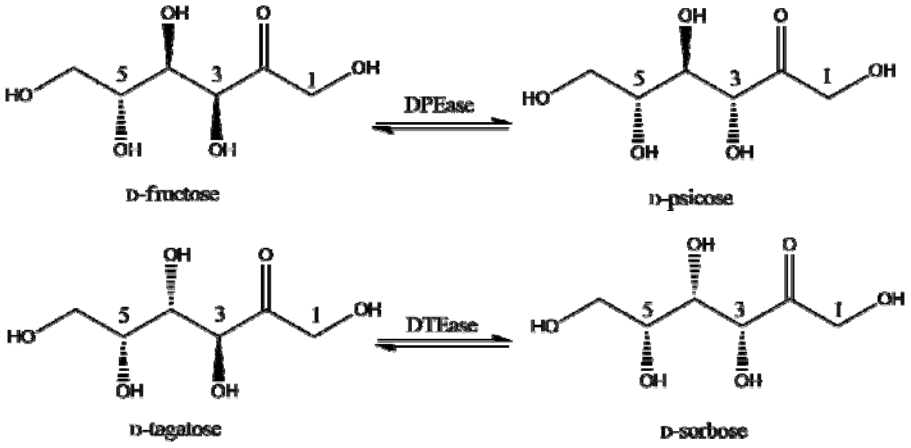

Figure 1. The epimerization reactions of D-fructose and D-tagatose catalyzed by *C. cellulolyticum* DPEase.

D-psicose, D-fructose and D-sorbose (Izumori, 1995), whereas the DPEase from *A. tumefaciens* showed the highest activity for D-psicose (Kim et al., 2006a). The optimal pH and temperature of *P. cichorii* DTEase are pH 7.5 and 60°C, whereas *A. tumefaciens* DPEase has pH 8.0 and 50°C. A third DTEase found in *Rhodobacter sphaeroides* has the highest activity to D-fructose. However, its bioconversion rate of D-psicose is 23% (40°C, pH 9.0), lower than the 32.9% rate of *A. tumefaciens* DPEase (Zhang et al., 2009). The DTEase/DPEase requires Mn^{2+} or Co^{2+} ion for fully enzymatic activity. Structures of *A. tumefaciens* DPEase and its complex with D-fructose have been solved (Kim et al., 2006b). Mutagenesis and structural analyses proved that some conserved active site residues are critical for activity (Kim et al., 2010a, 2010b). The structures of *P. cichorii* DTEase and its complex with D-tagatose and D-fructose have also been solved (Yoshida et al., 2007). These enzymes share several structural and functional features in common. However, the reason why DPEase has higher specificity for D-psicose than D-fructose remains unclear.

Clostridium cellulolyticum DPEase was recently characterized as a new member of DPEase (Mu et al., 2011). The optimal temperature for the enzyme reaction is 55°C. Different from *A. tumefaciens* DPEase, its activity is strictly dependent on metal ions and exhibits a maximal activity in the presence of Co^{2+} (100% activity) or Mn^{2+} (retained 92.7% activity). Moreover, *Clostridium cellulolyticum* DPEase has almost the same bioconversion rate of D-psicose (32%) as *A. tumefaciens* DPEase, but possesses a remarkable thermostability and the half-life is approaching 9.5 h at 55°C, much longer than the 8.9 min of *A. tumefaciens* DPEase (Kim et al., 2006a). The unique enzyme properties make *C. cellulolyticum* DPEase an attractive and potential candidate for further industrial application. In this study, to understand the relationship between the structure and function of *C. cellulolyticum* DPEase, we crystallized the apo-enzyme as well as the substrate-bound and product-bound complexes with D-psicose, D-fructose, D-tagatose and D-sorbose. The determination and analysis of these structures could give us more information about substrate specificity and catalytic mechanisms of *C. cellulolyticum* DPEase. The results not only provide us with more clues to the catalytic mechanism, but also with detailed structural information for future enzyme engineering to enhance the production of D-psicose from D-fructose.

RESULTS AND DISCUSSION

Overall structure

The crystals of *C. cellulolyticum* DPEase in this study all belong to the space group $P2_1$. To better understand the catalytic mechanism and substrate specificity, we also solved four different ketohexose complex structures. The apo-enzyme crystals are used to soak with four ketohexoses in the cryoprotectant. *C. cellulolyticum* DPEase crystallizes as a tetramer in an asymmetric unit and all soaked ketohexoses electron densities were clearly seen in each active site. The monomer structure of the *C. cellulolyticum* DPEase has eleven α-helices and eight β-strands that form a $(\beta/\alpha)_8$ TIM barrel fold with three additional short α-helices α1', α6' and α8' that follow β1, β6 and β8 (Fig. 2A and supplementary Fig. 1). A Mn^{2+} ion was observed in the apo-enzyme and all complex structures, bound to the active site. To investigate if any conformational change occurred upon substrate binding, the apo-form and substrate-bound complex structures are superimposed. The RMSD between apo-form DPEase and the structures in complex with D-psicose, D-fructose, D-tagatose and D-sorbose are 0.183 Å, 0.171 Å, 0.186 Å and 0.197 Å, respectively, for all Cα atoms. These results indicate that the ligand binding may not induce significant conformational change for overall structure.

C. cellulolyticum DPEase assembles into a tetramer (Fig. 2C). There are two different interfaces in a tetrameric DPEase: the dimeric interface between two subunits in a dimer (MolA-MolD, MolB-MolC) and the tetrameric interface between two dimers (Fig. 2C and 2D). The similarities

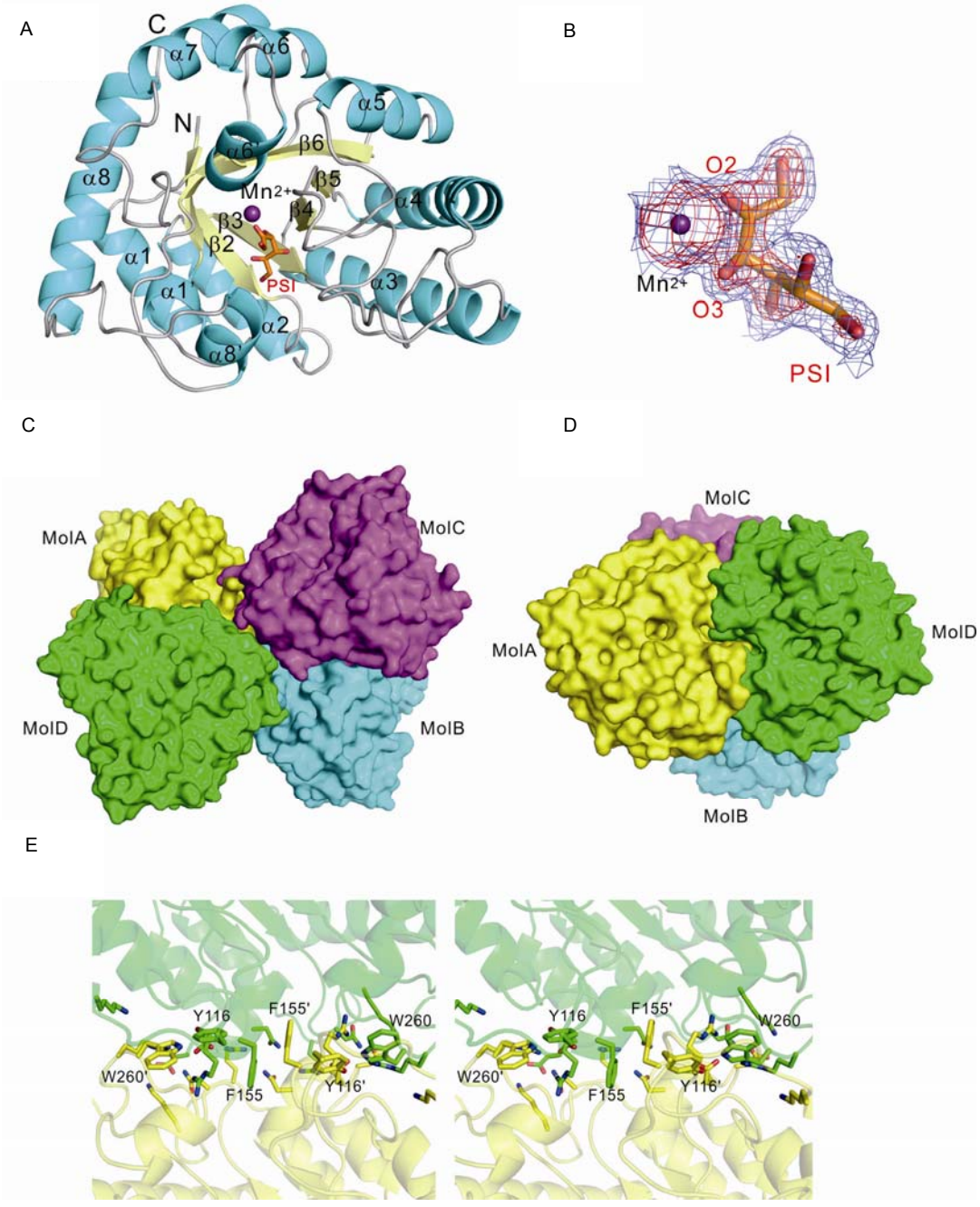

Figure 2. Structures of *C. cellulolyticum* DPEase. (A) The ribbon representation of the monomer of DPEase-PSI structure shows a TIM-barrel fold, with the α-helices (cyan) and β-strands (yellow) labeled. (B) The 2Fo-Fc electron density maps of the bound Mn^{2+} ion and D-fructose/D-psicose are shown at 1σ (blue) and 2.5σ (red) level. The Mn^{2+} ion is shown as a purple sphere. (C and D) The tetramer structure formed by MolA (green), MolB (cyan), MolC (magenta) and MolD (yellow) is shown in two orthogonal views. (E) Some residues at the interface between MolA and MolD are shown as stick and colored in green and yellow, respectively.

comparing our DPEase with *A. tumefaciens* DPEase and *P. cichorii* DTEase found were 60% and 42%, respectively. Compared with the structures of *P. cichorii* DTEase (2QUL) (Yoshida et al., 2007) and *A. tumefaciens* DPEase (2HK0) (Kim et al., 2006b), the monomers in *C. cellulolyticum* DPEase tetramer are assembled in a similar way as those in *A. tumefaciens* DPEase but not in *P. cichorii* DTEase. Although the monomers and dimers are similar, the two dimers of *P. cichorii* DTEase are related in a different way than those in the other two enzymes. Nevertheless, all monomers are

packed against each other by the closed sides of the barrel, making the active site fully accessible to the solvent. The dimeric interface between subunits A and D is shown in Fig. 2E. Eleven amino acid residues (Y116, K122, R154, N188, E190, D192, N214, K216, R222, W260, and R261) can form direct hydrogen bonds between the two subunits (totally forming 34 hydrogen bonds). The interactions for dimerization are quite extensive, resulting in interface solvent-accessible areas of 1406.4 Å^2 calculated by the PDBePISA website (http://www.ebi.ac.uk/msd-srv/prot_int/pistart.html). The detailed interactions are listed in supplementary Table 1. The dimer interface area of *C. cellulolyticum* DPEase is larger

Table 1 Summary of data processing and refinement statistics

Name	apo	DPEase-FRU	DPEase-PSI	DPEase-TAG	DPEase-SOR
PDB code	3VNI	3VNK	3VNJ	3VNL	3VNM
Data collection					
Resolution (Å)	25.00–1.98 (2.05–1.98)	25.00–2.02 (2.09–2.02)	25.00–2.08 (2.15–2.08)	25.00–2.15 (2.23–2.15)	25.00–2.12 (2.20–2.12)
Space group			$P2_1$		
Unit-cell					
a (Å)	79.8	80.0	79.9	80.4	79.9
b (Å)	115.4	115.2	115.5	115.4	115.2
c (Å)	91.6	91.4	91.6	91.5	91.6
β (º)	105.5	105.1	105.2	104.8	105.7
No. of reflections					
Measured	420021 (42248)	440319 (43797)	364610 (33206)	372966 (37594)	381511 (37770)
Unique	111299 (11118)	104455 (10428)	93519 (9224)	87319 (8743)	90274 (8993)
Completeness (%)	99.9 (100.0)	100 (100.0)	97.0 (96.6)	100.0 (100.0)	100.0 (100.0)
R_{merge} (%)[a]	8.6 (57.3)	5.8 (46.3)	5.5 (48.1)	5.1 (49.0)	5.3 (49.6)
Mean $I/\sigma(I)$	18.7 (2.6)	25.4 (3.5)	25.3 (3.1)	29.9 (3.4)	28.4 (3.4)
Multiplicity	3.8 (3.8)	4.2 (4.2)	3.9 (3.6)	4.3 (4.3)	4.2 (4.2)
Refinement					
No. reflections used	104262 (9460)	100158 (8972)	89106 (8033)	82961 (7541)	85232 (7485)
R_{work} (%)[b]	17.6 (26.9)	18.4 (27.7)	18.4 (28.0)	18.8 (30.7)	19.3 (29.8)
R_{free} (%)[b]	22.1 (31.7)	22.1 (30.1)	22.1 (30.1)	23.0 (34.0)	23.4 (32.5)
Geometry deviations					
Bond lengths (Å)	0.016	0.016	0.015	0.014	0.014
Bond angles (°)	1.630	1.820	1.780	1.670	1.670
No. of water molecules	1182	955	837	915	632
No. of ligands	Mn, 4	Mn, 8 D-fructose, 4	Mn, 4 D-psicose, 4	Mn, 4 D-tagatose, 4	Mn, 6 D-sorbose, 4
B-values (Å^2)					
Protein	28.9	35.9	40.5	45.2	47.5
Metal	40.5	40.9	30.2	34.1	48.5
Solvent	43.8	47.5	49.5	56.1	54.0
Ligand		40.1	42.5	56.8	48.1
Ramachandran plot (%)					
Most favored	96.25	95.73	96.73	95.64	95.31
Additionally allowed	3.40	3.66	3.75	3.31	3.83
Disallowed	0.35	0.61	0.52	1.05	0.96

Values in parentheses are for the highest resolution shell.

[a] $R_{merge} = \sum_{hkl}\sum_i |I_i(hkl) - \langle I(hkl)\rangle| \sum_{hkl}\sum_i I_i(hkl)$.

[b] $R_{work} = \sum|Fobs - Fcalc|/\sum Fobs$ and R_{free} is mathematically equivalent to R_{work} but measured over 5% of the data.

than that of *A. tumefaciens* DPEase (1380.6 Å^2). Interestingly, the *C. cellulolyticum* DPEase has higher optimal temperature and thermostability than *A. tumefaciens* DPEase (Mu et al., 2011). The optimal temperature for the *C. cellulolyticum* DPEase for maximum activity is 55°C *versus* 50°C for the *A. tumefaciens* DPEase (Mu et al., 2011). The *C. cellulolyticum* DPEase also has higher thermostability than the *A. tumefaciens* DPEase (55°C, 9.5 h for the *C. cellulolyticum* DPEase and 50°C, 8.9 min for the *A. tumefaciens* DPEase). The stronger interactions and tighter tetramer formation may contribute to the higher thermostability and optimal temperature.

Active site and substrate binding

A Mn^{2+} ion in coordination with four residues (E150, D183, H209 and E244) and two water molecules is seen in the active site of *C. cellulolyticum* apo-form DPEase (supplementary Fig. 2). Although there is no major conformational change between the apo-form and substrate/product complex structures, there are slight alterations in the active site structure upon binding to substrate/product. For example, from the D-psicose complex structure, some hydrophobic residues in the active site (e.g. Y6, F246, W14, and W112) moved toward the bound D-psicose (Fig. 3A). Moreover, conformational changes in some polar residues (E150, E156, H208 and E144) occurred to form the hydrogen bonds with D-psicose. The observed eclipse configuration of O2 and O3 for bound D-psicose and D-fructose or D-tagatose and D-sorbose indicates a rotation of the C2-C3 bond (Fig. 3B).

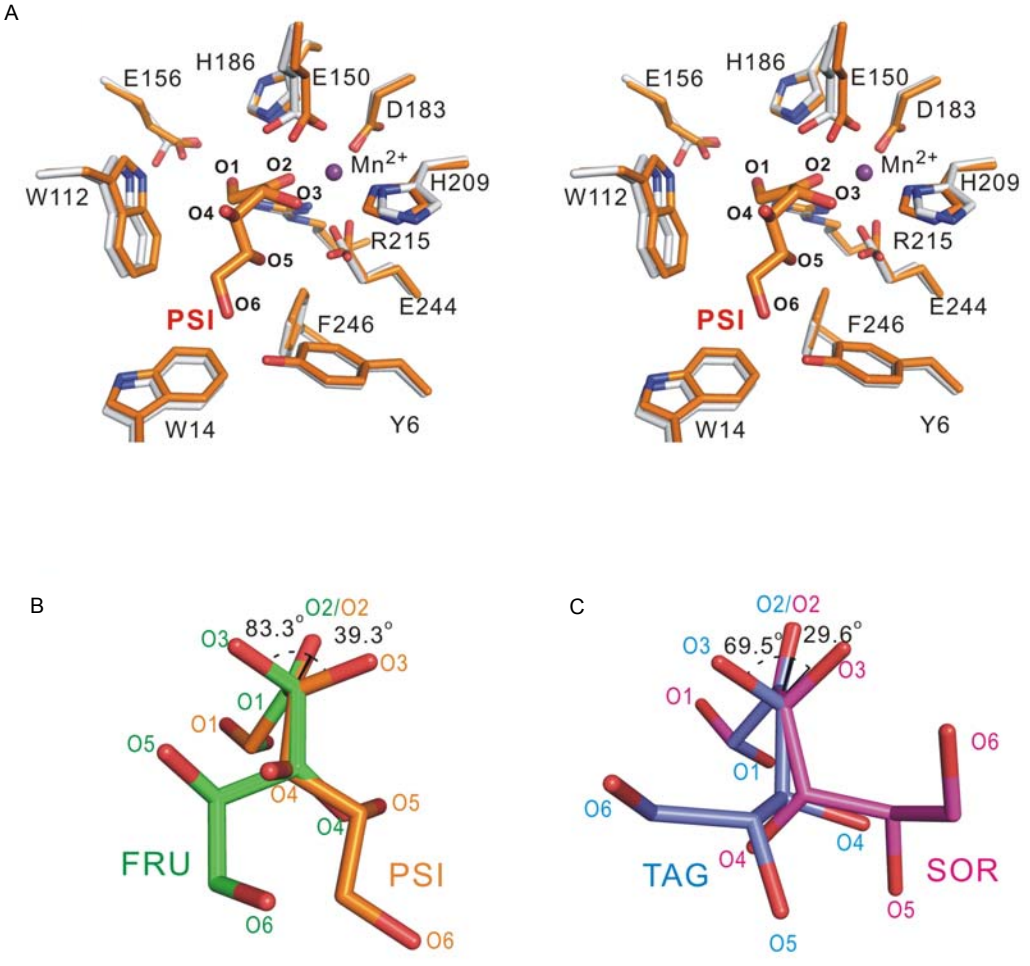

Figure 3. Comparison of the apo-enzyme and substrates/products bound structures. (A) Structure superimposition of the active site of apo-DPEase and D-psicose bound complex is shown by stick models with carbon atoms colored in gray and orange, respectively. The purple sphere represents Mn^{2+}. The oxygen atoms in the bound D-psicose are labeled. (B) The superimposition of D-psicose and D-fructose with paired C2-C3 atoms. D-psicose and D-fructose are colored in orange and green, respectively. (C) The superimposition of D-tagatose and D-sorbose with paired C2-C3 atoms. D-tagatose and D-sorbose are colored in blue and magenta, respectively.

The electron density map of each ketohexose clearly shows that the carbonyl oxygen O2 and hydroxyl group O3 of each ketohexose are coordinated with Mn^{2+} (Fig. 2B and supplementary Fig. 3). The detailed interactions between the active site residues of *C. cellulolyticum* DPEase with D-psicose, D-fructose, D-tagatose and D-sorbose are depicted in Fig. 4. From the DPEase-PSI structure (Fig. 4A), the O1 of D-psicose makes hydrogen bonds with E156, H186 and R215. The O2 makes hydrogen bonds with E150, D183 and H186. E150 and E244 make hydrogen bonds with O3 and play an important role in an epimerization reaction at the C3 position. The O4, O5 and O6 make hydrogen bonds with H209, E244 and Y6, respectively. From DPEase-FRU structure (Fig. 4B), the O1 of D-fructose makes hydrogen bonds with E156 and R215. The O2 makes hydrogen bonds with D183, R215 and E244. Glu150 makes two hydrogen bonds with O3. The O4 and O6 make hydrogen bonds with H209 and Y6, respectively. The detailed hydrogen bonding interactions of each ketohexose complex structure are shown in supplementary Table 2.

Epimerization activities of the *C. cellulolyticum* DPEase and other DPEase/DTEase for various substrates are very different (Izumori, 1995; Kim et al., 2006a; Zhang et al., 2009). The substrate specificity of the *C. cellulolyticum* DPEase was similar to the *A. tumefaciens* DPEase, and is somewhat different from the *P. cichorii* DTEase and the *R. sphaeroides* DTEase. The *C. cellulolyticum* DPEase prefers using D-psicose to D-fructose, D-tagatose and D-sorbose in a decreasing order, and the relative activities are 100%, 48.2%, 4.9% and 0.9%, respectively (Mu et al., 2011). The epimerization activities of the *C. cellulolyticum* DPEase for D-tagatose and D-sorbose are very low when compared to that for D-psicose. Previous kinetic studies have shown that the k_{cat}/K_m of the *C. cellulolyticum* DPEase for D-psicose was 2.97-fold higher than that for D-fructose and the K_m of the *C. cellulolyticum* DPEase for D-psicose was 3.52-fold lower than that for D-fructose (Mu et al., 2011). From our refined *C. cellulolyticum* DPEase complex structures, that the affinity for D-psicose was higher than D-fructose may be attributed to the formation of more hydrogen bonds between D-psicose and the enzyme. Based on our *C. cellulolyticum* DPEase structures in complex with D-tagatose and D-sorbose, there are fewer hydrogen bonds formed between the enzyme and these sugars (D-tagatose and D-sorbose) (Fig. 4C and 4D). When comparing four substrate/product complex structures carefully, Y6 and E244 may be very important for binding and E244 may also play an important role in catalysis (will be mentioned later). To figure out if Y6 and E244 are important for substrate/product binding, the total hydrogen bonds formed from these four complex structures were analyzed. For the D-psicose binding, there are four hydrogen bonds formed (E244 provides 3 direct hydrogen bonds and Y6 provides 1 hydrogen bond). For the D-fructose binding, there are three hydrogen bonds formed (Y6 provides 1 hydrogen bond and E244 provides 2 direct hydrogen bonds). For the D-tagatose and D-sorbose binding, there are only one and two direct hydrogen bonds formed by Y6 and E244 residues, respectively (Fig. 4C and 4D). As mentioned above, the *C. cellulolyticum* DPEase has very low relative activity against D-tagatose (4.9%) and D-sorbose (0.9%). Although there was an additional hydrogen bond for D-sorbose compared with D-tagatose, Y6 did not bind to the O6 as for the D-tagatose and D-sorbose. That might not be the adequate configuration/orientation for Y6 to bind with and may cause the enzyme to show the worst activity for D-sorbose.

Catalytic mechanism

Based on the proposed catalytic mechanism of *A. tumefaciens* DPEase, one of the two Glu residues (E150 and E244) coordinated with the Mn^{2+} metal first removes a proton from C3 to generate a cis-enediolate intermediate, and then the other Glu residue protonates C3 on the opposite side. However, there was no direct structural information to support this hypothesis before. In this study, we successfully determined both substrate-bound and product-bound complex structures of *C. cellulolyticum* DPEase (Fig. 5). The distance between E244 of the enzyme and C3 of the bound D-fructose is 2.6 Å and this indicates that the E244 firstly removes a proton from C3 and then E150 pronates C3 on the opposite side. However, the distance between E150 of the enzyme and C3 of the bound D-psicose is 2.8 Å and the reverse reaction would involve deprotonation/protonation by E150/E244, respectively. Our substrate- and product-bound structures provide a more clear view to the question of how the ionization state of E150 and E244 is altered during epimerization by *C. cellulolyticum* DPEase.

The apo-enzyme and complex structures presented in this study will provide us with a structural basis for protein engineering and may further improve the enzyme's relative activity and yield of bioproduction from D-fructose to D-psicose. As we know, D-tagatose is also an important rare sugar and can be widely used in a variety of industries (e.g. food industry). It has many health benefits, such as promotion of weight loss and suppression of glycemic effect (Oh, 2007). Based on our structural information, it might also be possible to engineer this enzyme to increase the relative activity and improve the production of D-tagatose from D-sorbose by site directed mutagenesis to better recognize the 4, 5, 6-OH of D-sorbose.

MATERIALS AND METHODS

Protein expression and purification

The full-length nucleotide sequence of the DPE gene from *C. cellulolyticum* H10 was synthesized and cloned into the pET-21a vector. Then the recombinant *C. cellulolyticum* DPEase plasmid was transformed into *E. coli* BL21 (DE3) for protein expression. The *E. coli*

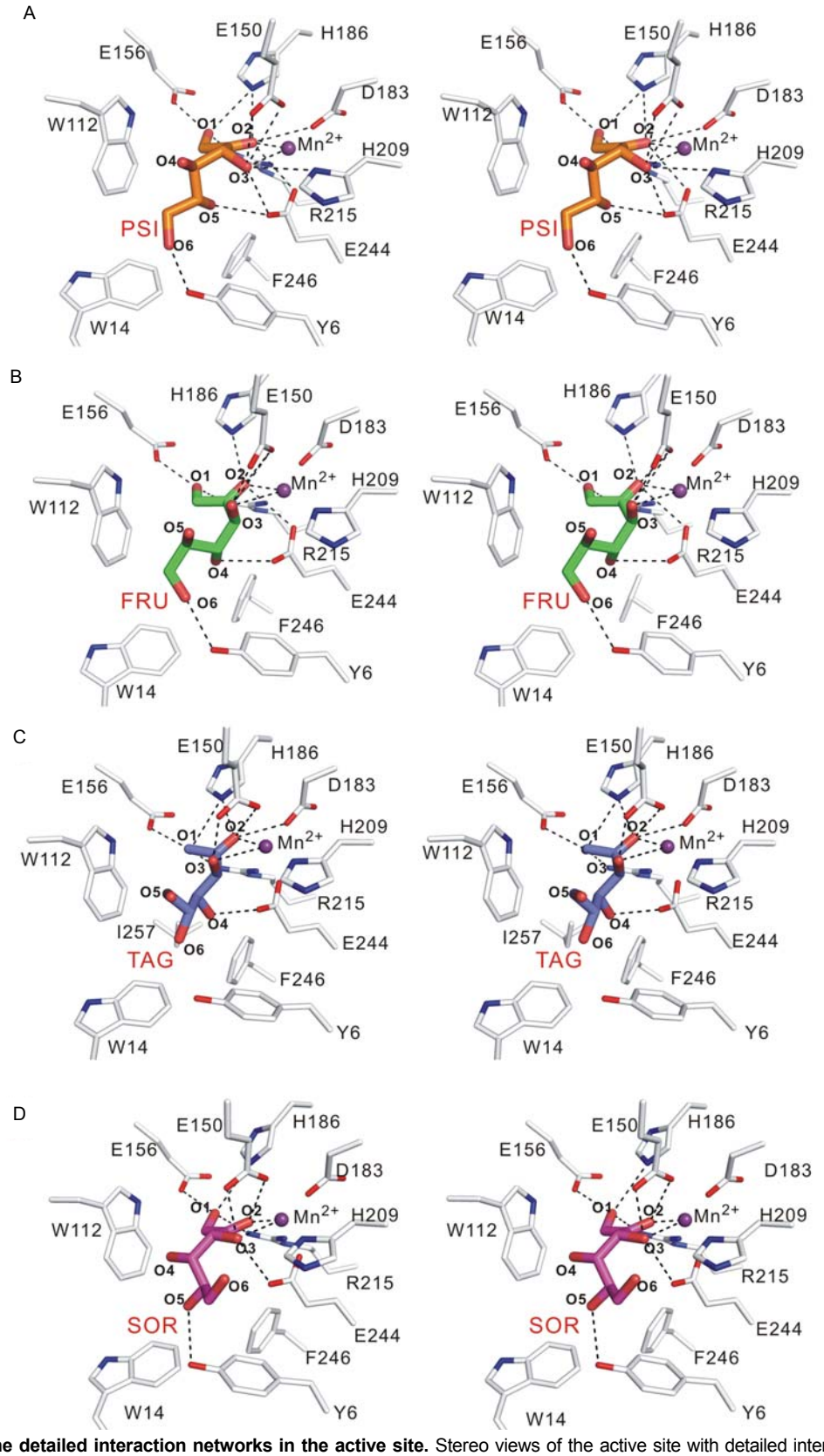

Figure 4. The detailed interaction networks in the active site. Stereo views of the active site with detailed interactions in the ketohexose-bound complex structures for (A) D-psicose, (B) D-fructose, (C) D-tagatose and (D) D-sorbose are shown. Hydrogen bonds with distances of less than 3.2 Å are shown as black dashed lines.

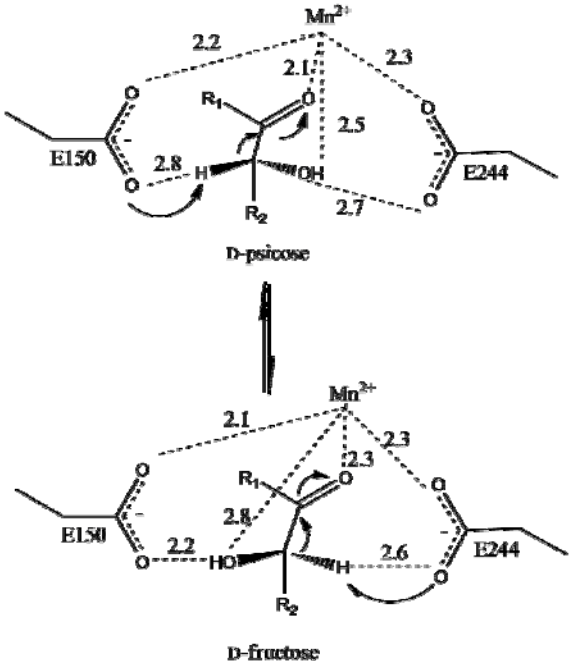

Figure 5. The catalytic mechanism of *C. cellulolyticum* DPEase. The hydrogen bond distances are measured from the DPEase-psicose and DPEase-fructose complex structures.

cells expressing *C. cellulolyticum* DPEase were harvested from culture broth by centrifugation at 6000 rpm for 10 min at 4°C, and suspended in a lysis buffer (25 mmol/L Tris–HCl, 300 mmol/L NaCl, 40 mmol/L imidazole, pH 8.0). The crude extract was applied to a 5-mL HisTrap HP affinity chromatography column (GE Healthcare BioSciences) equilibrated with binding buffer (25 mmol/L Tris–HCl, 300 mmol/L NaCl, 40 mmol/L imidazole, pH 8.0). The bound protein was eluted with a linear gradient between 40 to 250 mmol/L imidazole and the protein was eluted at about 150 mmol/L imidazole concentration. The purified protein solution from HisTrap HP affinity chromatography column was dialyzed to 50 mmol/L sodium phosphate buffer (pH 6.5) and then loaded onto a Source 15Q anion exchange chromatography column (GE Healthcare BioSciences). The protein was eluted with a linear gradient between 0 to 500 mmol/L NaCl and the protein was eluted at about 200–250 mmol/L NaCl concentration. The protein was further dialyzed and concentrated to 10 mg/mL concentration in 25 mmol/L Tris–HCl, 150 mmol/L NaCl, pH 7.5. All purification steps were carried out with ÄKTA purifier™ 100 system. The purity (> 95%) of *C. cellulolyticum* DPEase was checked by SDS-PAGE.

Crystallization and data collection

C. cellulolyticum DPEase was crystallized using the sitting drop method from Hampton Research (Laguna Niguel, CA) by mixing 2 μL of the protein solution (10 mg/mL in 25 mmol/L Tris–HCl, 150 mmol/L NaCl, pH 7.5) and 2 μL of the mother liquor, equilibrated with 500 μL of the mother liquor at room temperature. The optimal crystallization conditions for all crystals mentioned here are modified as 0.2 mol/L tri-sodium citrate dehydrate pH 8.2, 17%–20% Polyethylene Glycol 3350. The data set of wild-type DPEase was collected at beam line BL17U of the Shanghai Synchrotron Radiation Facility (SSRF) in Shanghai, China. The crystals of DPEase in complex with D-fructose (DPEase-FRU), D-psicose (DPEase-PSI), D-tagatose (DPEase-TAG) and D-sorbose (DPEase-SOR) were obtained by soaking the native DPEase crystal with 10 mmol/L D-fructose, D-psicose, D-tagatose or D-sorbose in cryoprotectant (0.2 mol/L tri-sodium citrate dehydrate pH 8.2, 18% Polyethylene Glycol 3350, 0.5 mol/L $MnCl_2$, and 20% glycerol). All complex data sets were collected at beam line 13C1 of the National Synchrotron Radiation Research Center (NSRRC) in Taiwan, China. Diffraction data was processed and scaled by HKL2000 (Otwinowski and Minor, 1997). The apo-enzyme and four substrates/products complex structures are collected at 1.98 to 2.15 Å resolution. The statistics of data collection and refinement are shown in Table 1.

Structure determination and refinement

The initial phase of *C. cellulolyticum* DPEase was determined by using molecular replacement method (MR) with PHASER (McCoy et al., 2007) in CCP4 program suite (Potterton et al., 2003), and the *A. tumefaciens* DPEase (2HK0) was used as the searching model. The crystals all belong to $P2_1$ space group and there are four molecules in an asymmetric unit. Iterative cycles of manual model building are used by Coot (Emsley and Cowtan, 2004), MIFit (D.E., 2004) and CNS (Brünger et al., 1998). The DPEase structures in complex with D-fructose, D-psicose, D-tagatose and D-sorbose were solved by molecular replacement, using the refined apo-DPEase as the search model. These models were further refined with CNS and waters and substrates were added by using MIFit. Detailed refinement statistics are shown in Table 1.

ACKNOWLEDGEMENTS

This work was supported by grants from Science and Technology Projects of Tianjin (No. 10YFYBJC00100), National High Technology Research and Development Program of China (863 Project) (Grant No. 2012AA021503), Visiting Professorships for Senior International Scientists (No. 2010T1S4) and One Hundred Talents Project of The Chinese Academy of Sciences to RTG.

The synchrotron data collection was conducted at beam line BL13C1 of NSRRC (National Synchrotron Radiation Research Center, Taiwan, China) supported by the National Science Council (NSC) (Taiwan, China), and at beam line BL17U of SSRF (Shanghai, China).

Supplementary material is available in the online version of this article at http://dx.doi.org/10.1007/s13238-012-2026-5 and is accessible for authorized users.

REFERENCES

Brünger, A.T., Adams, P.D., Clore, G.M., DeLano, W.L., Gros, P.,

Grosse-Kunstleve, R.W., Jiang, J.-S., Kuszewski, J., Nilges, M., Pannu, N.S., et al. (1998). Crystallography & NMR system: A new software suite for macromolecular structure determination. Acta Crystallogr D Biol Crystallogr 54, 905–921.

Granström, T.B., Takata, G., Tokuda, M., and Izumori, K. (2004). Izumoring: a novel and complete strategy for bioproduction of rare sugars. J Biosci Bioeng 97, 89–94.

Itoh, H., Khan, A.R., Tajima, S., Hayakawa, S., and Izumori, K. (1994). Purification and characterization of D-tagatose 3-epimerase from Pseudomonas sp. ST-24. Biosci Biotechnol Biochem 57, 1037–1039.

Izumori, K. (1995). Preparation of D-psicose from D-fructose by immobilized D-tagagtose-3-epimerase. J Ferment Bioeng 80, 101–103.

Izumori, K. (2002). Bioproduction strategies for rare hexose sugars. Naturwissenschaften 89, 120–124.

Kim, H.-J., Hyun, E.-K., Kim, Y.-S., Lee, Y.-J., and Oh, D.-K. (2006a). Characterization of an Agrobacterium tumefaciens D-psicose 3-epimerase that converts D-fructose to D-psicose. Appl Environ Microbiol 72, 981–985.

Kim, H.-J., Lim, B.-C., Yeom, S.-J., Kim, Y.-S., Kim, D., and Oh, D.-K. (2010a). Roles of Ile66 and Ala107 of D-psicose 3-epimerase from *Agrobacterium tumefaciens* in binding O6 of its substrate, D-fructose. Biotechnol Lett 32, 113–118.

Kim, H.-J., Yeom, S.-J., Kim, K., Rhee, S., Kim, D., and Oh, D.-K. (2010b). Mutational analysis of the active site residues of a D: -psicose 3-epimerase from *Agrobacterium tumefaciens*. Biotechnol Lett 32, 261–268.

Kim, K., Kim, H.-J., Oh, D.-K., Cha, S.-S., and Rhee, S. (2006b). Crystal structure of D-psicose 3-epimerase from Agrobacterium tumefaciens and its complex with true substrate D-fructose: a pivotal role of metal in catalysis, an active site for the non-phosphorylated substrate, and its conformational changes. J Mol Biol 361, 920–931.

Kim, N.-H., Kim, H.-J., Kang, D.-I., Jeong, K.-W., Lee, J.-K., Kim, Y., and Oh, D.-K. (2008). Conversion shift of D-fructose to D-psicose for enzyme-catalyzed epimerization by addition of borate. Appl Environ Microbiol 74, 3008–3013.

Matsuo, T., Baba, Y., Hashiguchi, M., Takeshita, K., Izumori, K., and Suzuki, H. (2001). Dietary D-psicose, a C-3 epimer of D-fructose, suppresses the activity of hepatic lipogenic enzymes in rats. Asia Pac J Clin Nutr 10, 233–237.

Matsuo, T., and Izumori, K. (2006). Effects of dietary D-psicose on diurnal variation in plasma glucose and insulin concentrations of rats. Biosci Biotechnol Biochem 70, 2081–2085.

Matsuo, T., Suzuki, H., Hashiguchi, M., and Izumori, K. (2002). D-psicose is a rare sugar that provides no energy to growing rats. J Nutr Sci Vitaminol (Tokyo) 48, 77–80.

McCoy, A.J., Grosse-Kunstleve, R.W., Adams, P.D., Winn, M.D., Storoni, L.C., and Read, R.J. (2007). Phaser crystallographic software. J Appl Crystallogr 40, 658–674.

McRee, D.E. (2004). Differential evolution for protein crystallographic optimizations. Acta Crystallogr D Biol Crystallogr 60, 2276–2279.

Mu, W., Chu, F., Xing, Q., Yu, S., Zhou, L., and Jiang, B. (2011). Cloning, expression, and characterization of a D-psicose 3-epimerase from Clostridium cellulolyticum H10. J Agric Food Chem 59, 7785–7792.

Oh, D.-K. (2007). Tagatose: properties, applications, and biotechnological processes. Appl Microbiol Biotechnol 76, 1–8.

Otwinowski, Z., and Minor, W. (1997). Processing of X-ray diffraction data collected in oscillation mode. In: Methods in enzymology, macromolecular crystallography, part A. Carter C.W., Jr. and Sweet R. M. eds. New York: Academic Press, 307–326.

Emsley, P., and Cowtan, C. (2004). Coot: model-building tools for molecular graphics. Acta Crystallogr D Biol Crystallogr 60, 2126–2132.

Potterton, E., Briggs, P., Turkenburg, M., and Dodson, E. (2003). A graphical user interface to the CCP4 program suite. Acta Crystallogr D Biol Crystallogr 59, 1131–1137.

Samuel, J., and Tanner, M.E. (2002). Mechanistic aspects of enzymatic carbohydrate epimerization. Nat Prod Rep 19, 261–277.

Yoshida, H., Yamada, M., Nishitani, T., Takada, G., Izumori, K., and Kamitori, S. (2007). Crystal structures of D-tagatose 3-epimerase from Pseudomonas cichorii and its complexes with D-tagatose and D-fructose. J Mol Biol 374, 443–453.

Zhang, L., Mu, W., Jiang, B., and Zhang, T. (2009). Characterization of D-tagatose-3-epimerase from *Rhodobacter sphaeroides* that converts D-fructose into D-psicose. Biotechnol Lett 31, 857–862.

